MICROSEISMIC INVESTIGATION OF THE KIJIYAMA-SHITANOTAI GEOTHERMAL FIELD

Alan Lucas[1], Tatsuya Sato[2] , Tomohiro Takahashi[3], Koushirou Takanashi[2] and Hylton White[1]

[1]International Earth Sciences IESE Ltd (IESE) 29 East St, Auckland, New Zealand

[2]Geothermal Energy Research & Development Co., Ltd., Japan

[3]Touhoku Sustainable & Renewable Energy Co. Inc., Miyagi, Japan.

Alan.lucas@iese.co.nz

Keywords: *Microseismicity, Shear Wave Splitting, Geothermal, Exploration*

ABSTRACT

In 2012 and 2017, temporary seismic networks were installed at a Kijiyama-Shitanotai geothermal field, Akita prefecture, Japan. Microseismic data was gathered using these networks for three months in each case. The networks were located in different areas of the geothermal system. The data was analyzed to identified of 499 local micro-earthquakes in 2017 and 475 in 2012 (a total of 974). From this data a velocity model was derived, and the earthquakes located. The shear waves recorded were analyzed for shear wave splitting (SWS). The SWS splitting results were used to derive a three-dimensional crack density model and polarization direction. The SWS result indicates a high in crack density and NE striking fractures in the north of the seismic network and NW striking in the south.

1. INTRODUCTION

This report details work done by the Geothermal Energy Research & Development Co., Ltd (GERD) and International Earth Sciences IESE Ltd (IESE) staff, in installing a microseismic network at Kijiyama-Shitanotai geothermal field in Japan. The geothermal field currently has a Geothermal Power Plant with a design capacity of 28.8 MWe The report focuses on the acquisition, description and analysis of micro-earthquake data acquired.

2. NETWORK INSTALLATION AND DATA ACQUISITION

Two seismic networks were installed by Geothermal Energy Research & Development Co., Ltd (GERD) and International Earth Sciences IESE Ltd (IESE), staff in the Kijiyama-Shitanotai Geothermal system. The first was installed in October 2012 (stations J01 to J15, Figure 1) and the second in June 2017 (stations J16 to J30, Figure 1). Both networks operated for a approximate period of three months and both networks consisted of 15 seismic stations. The locations of the all but two of the stations in each network were different. The 2012 network focused on the NW of the area of interest and the 2017 on the South. Two stations (J16 and J18) were co-located so that the two networks would overlap.

In the 2012 deployment, Geospace MiniSeisMonitor sensors, with a corner frequency of 2.0 Hz were utilized. Data was recorded on Reftek 130-01 Data Acquisition Systems (DAS), and sampled at a rate of 250 sps. In the 2017 deployment, nine of the stations used were the same as the 2012 deployment. Two of the stations used IESE manufactured F160B-4.5, with a corner frequency of 4.5 Hz. Four of the stations utilized the Reftek GOES system, which samples at 500 sps and contains the same sensors used in the Geospace MiniSeisMonitor. Power was supplied using batteries at each station which were manually changed for charging . The lower sampling rate on the Reftek 130 stations was chosen due to its lower power consumption.

The sensors at each station recorded in three perpendicular axis(vertical, magnetic north-facing, magnetic east-facing). These units were buried, typically half a meter below the surface where possible. Timing was provided via a GPS satellite link.

3. RESULTS

The raw seismic waveform data was processed by running a triggering algorithm based on an STA/LTA approach [Ambuter, B.P., and Solomon S.C.]. The result of this is Event Files which contain a short segment of the raw data for inspection. For data gathered by the 2017 Kijiyama-Shitanotai network, a total 18900 events were manually inspected to investigate if they represented an earthquake. If an earthquake is identified, then the arrival times of the P-wave and S-wave phases were stored. These phase picks were then used to locate the earthquake, using the USGS Hypoinverse software [Klein, F.W.]. A local velocity model was derived from the data gathered using a genetic algorithm approach [de Vasconcelos Lopes, A.E., and Assumpção, M.].

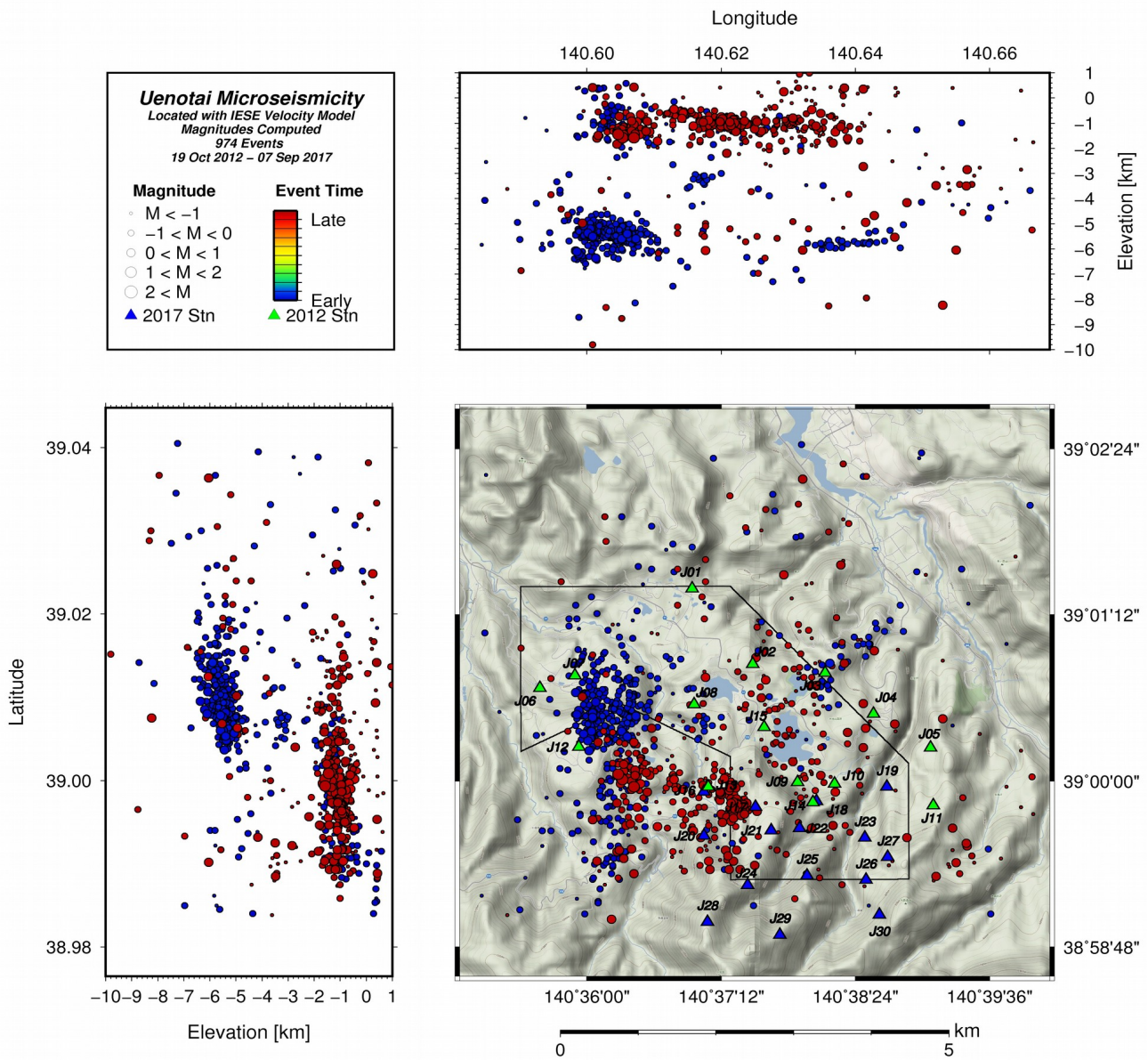

Figure 1: The local event catalog including events which were detected by the 2012 network. Earthquakes are sized by Magnitude and colored by the date they occurred (blue = 2012 and red = 2017). Blue (2017) And Green (2012) triangles indicate stations installed. The black boundary represents the area of interest. The map plot in this figure has the same boundaries as that used in Figure 2 and Figure 4.

3.1 Micro-Earthquake Locations

A total of 974 earthquakes were identified within the local area (see Figure 1). A further 276 earthquakes were identified with locations greater than 5km from the network, typically to the East. Some of these earthquakes had magnitudes large enough to be identified in the Japan Meteorological Agency (JMA) Unified Hypocenter Catalogue [Obara K., Kasahara K., Hori S. and Okada Y.]. These co-identified earthquakes were used to calibrate the Kijiyama-Shitanotai network magnitudes to that calculated in the JMA catalog.

The local micro-earthquake locations can be split into two broad groups: deep (-5 to -6 km) and shallow (-1 to -2 km). The deep group is dominated by earthquakes identified by the 2012 network and the shallow by the 2017 (see Figure 1). Magnitude's observed are generally below 1M_w.

3.2 Shear Wave Splitting

Shear wave splitting (SWS) is caused when a randomly polarized shear wave propagating to the surface encounters an area where the shear wave velocity is anisotropic [Lou M.,

Shalev E., and Malin P.E.]. There are two proposed causes of this anisotropy: parallel aligned fluid-filled fractures and aligned crystal structure. In near-surface applications such as in this study, shear wave splitting is assumed to be caused by parallel aligned fluid-filled fractures [Rial, J.A., Maya E., and Ming Y.]. SWS analysis produces two types of observation for each earthquake-station pair: Splitting fast wave polarisation and SWS delay time.

Methods for measuring shear wave splitting parameters (fast wave polarisation and SWS delay time) often involve multiple measurements of the similarity two potentially split shear waves [Crampin, S, and Yuan G]. The method used for this investigation involves the selection of multiples windows with different polarisations and time delays. The time delay and polarisation are corrected for and the linearity of the shear wave calculated. The quality of the measurement is calculated using the linearity. Results shown in subsequent sections are the highest quality observations with qualities above 0.4.

3.3 Splitting Fast Wave Polarisation

The Splitting orientations are a measure of the orientation of the fast shear wave polarisation. This orientation is often thought of as an indicator of subsurface fracture orientation. The fractures are thought to be parallel in strike to the fast wave polarisation. It is important to note that polarisations many indicate fracture orientation at any point along the ray between the earthquake and the recording station. It is also important to note that under some scenarios fast polarisation directions do not directly indicate fracture strike

The Kijiyama-Shitanotai seismic network observed multiple fast wave polarisation directions (Figure 2). Results suggest that the fracture zones generating SWS observations are complex, with no single, consistent splitting direction being observed across all stations in the field. The two dominant directions are NE and NW, which will be discussed further below.

An overall trend of NE-SW polarizations is observed at many of the stations to the SE and the N of the network. The earthquakes corresponding to the SE observations are in the western part of the network. The path the shear waves take is across the northern half of the 2017 network (in the area of J17 and J18), implying that the fluid-filled fracture systems in that area are of an NE-SW orientation (Assuming the SWS is entirely attributed to fractures).

Stations J28, J06 and J12 show an NW trend in the fast wave polarisations (Figure 2), trend is observed in both the 2012 and 2017 deployments. The earthquakes generating this fast direction occur as part of two clusters located near J16 and J07 respectively. SWS with a single clear polarisation, as is being analyzed here, is assumed to occur when a shear wave passes through a fracture zone with a single dominate orientation. As some the NE and NW orientations come from the same general area of earthquake locations (near J16), it is implied that the fracture systems generating SWS are not in that area.

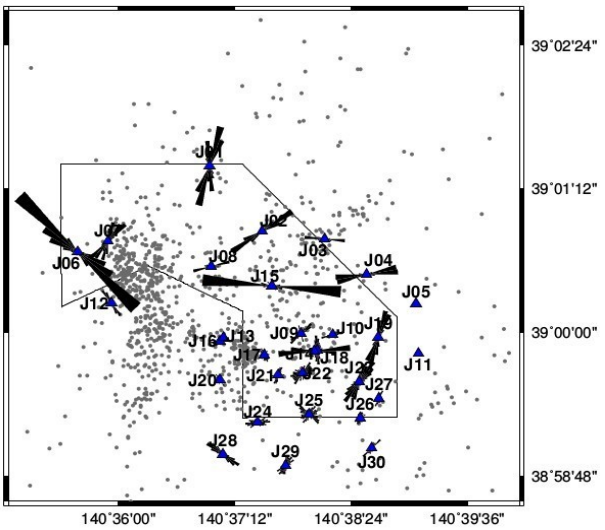

Figure 2: Shear wave splitting fast wave orientations for the Kijiyama-Shitanotai data. Seismic stations are indicated by blue triangles and the area of interest is indicated by a black line. The boundaries of this plot are the same as that used in Figure 1 (map) and Figure 4.

The station J14 of the 2012 network is located at a similar location to that of J18. The fast wave polarisation observed at these two stations is different by 90 degrees. The earthquake sources for these polarisation directions are different. The E fast wave polarizations earthquakes locate near J07 (like J15). The N fast wave polarizations earthquakes locate near J16. The differences in source locations of the two directions implies that the polarisation source is not local to the station, and occurs at some point along the different paths the seismic waves take.

3.4 Crack Density Inversion

The SWS delay time between the fast and slow shear waves is inverted together with the shear-wave-velocity to determine crack-density. Crack density is defined as the number of cracks in a unit volume multiplied by the crack radius cubed (a unit less number). A crack is defined as a thin water filled disk. IESE uses a Crack density inversion algorithm based on a relationship between time delay, crack density and angle of incidence of the ray and fracture [Crampin, S, and Yuan G.].

Inversion results for the entire (2012 and 2017) data set are displayed in Figure 3. Given the small number of SWS observations, the decision was made to combine the 2012 and 2017 data sets, and only calculate the result for the combined data. Slices of the crack density model and hit number at a constant depth are displayed. The crack density model is unconstrained in areas where the hit number is zero. Thus the crack density model is masked in areas where the hit plot is zero.

The inversion results show a maximum in crack density at shallow depths (at sea level) located in the middle of the network. The highest crack density values of 0.08 are observed in this area; this is comparable to some other areas, for example, 0.08 for an Indonesian field and 0.08 – 1.0 at Puna in Hawaii. This crack density anomaly decreases in intensity with depth, although the values >0.07 are higher than the background (of ~0.04). At a depth of 3 km and below the inversion, the result becomes less constrained as the ray coverage begins to be reduced due to fewer earthquakes below this depth. A low in crack density of 0.05 (relative to the 0.08 mentioned earlier) is seen in the middle of the network.

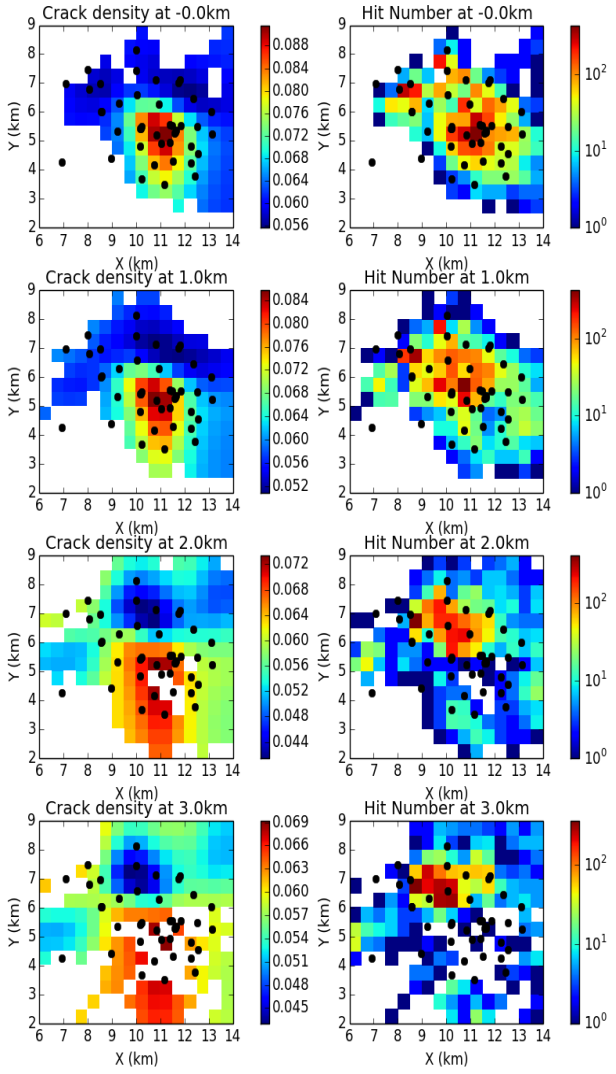

Figure 3: Crack density inversion results. The left colour shows the crack density (with red being high crack density) at a fixed depth (relative to sea level, indicated in the plot title) and the right the corresponding hit plot. Crack density is a unit less number. Hit plots are in number of rays. Black circles are seismic stations.

4. DISCUSSION

The earthquake locations do not follow any strong linear trends that lend themselves to a fault interpretation. The earthquake locations do not seem to follow any of the mapped fault systems either (Figure 4). It is unclear if this is because the earthquakes are a result of deeper unmapped structures, their locations are not structurally constrained, or that their location resolution is to low.

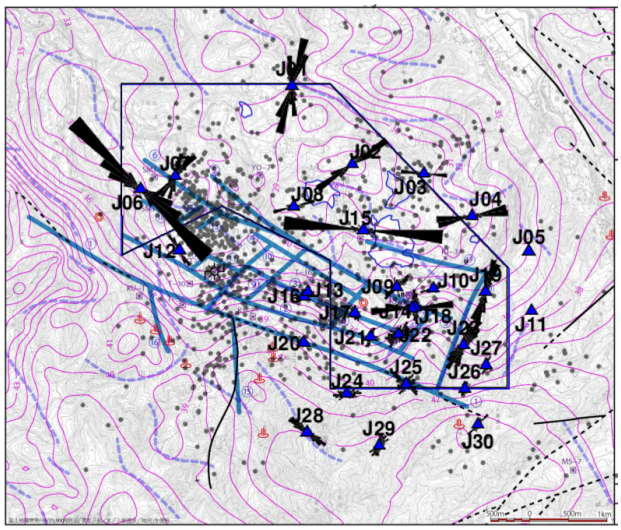

Figure 4: Shear wave splitting fast wave polarisation rose diagrams (black) and earthquakes results (gray circles). These are overlaid on a image displaying faults (blue lines) and Bouguer anomaly (contours). Blue triangles indicate seismic stations installed. The black boundary represents the area of interest. Red symbols indicate surface manifestations of hot springs. The boundaries of this plot are the same as that used in Figure 1 (map) and Figure 2.

The NE direction Shear Wave Splitting (SWS) fast polarizations observed at some stations align well with fracture systems that are present in surface mapped geology. As discussed, this implies an NE orientation to fluid filled fractures in the east of the network. Stations to the south of the network display NW fast polarizations. These NW polarizations correlate well with the large-scale fault systems seen in the structural geological data. The crack density inversion results identify an intense anomaly in the center of the network, near J24. This does not correlate strongly with either the earthquake locations or the mapped faults.

5. CONCLUSIONS

Two deployments of 15 seismic stations have been successfully installed in the Kijiyama-Shitanotai geothermal field, Akita prefecture, Japan. A total of 974 earthquakes were identified within the local area, a further 276 regional earthquakes were identified during the two deployments. Shear wave splitting (SWS) analysis has been conducted on the data gathered. This indicated both NE and NW fast wave polarisation directions. These directions correlate well in some areas with the mapped fault systems. The crack density inversion results identify an intense anomaly in the north of the 2017 network, in the area of stations J15, J16 and J17.

ACKNOWLEDGEMENT

IESE and GERD wish to acknowledge the permission of the Touhoku Sustainable & Renewable Energy Co in allowing the publication of these results.

References

Ambuter, B.P., and Solomon S.C.: *An event recording system for monitoring small earthquakes.* (in Indonesian). Bulletin of the Seismological Society of America, 64(4), pp 1181-1188. (1974).

Klein, F.W.: *A User's Guide to HYPOINVERSE-2000, a Fortran Program to Solve for Earthquake Locations and Magnitudes.* (USGS Open File Report 02-171 revised, V1.37. (2012).

de Vasconcelos Lopes, A.E., and Assumpção, M.: *Genetic algorithm inversion of the average 1D crustal structure using local and regional earthquakes.* Computers & Geosciences, 37(9), pp 1372-1380. (2011).

Obara K., Kasahara K., Hori S. and Okada Y.: A *densely distributed high-sensitivity seismograph network in Japan: Hi-net by National Research Institute for Earth Science and Disaster Prevention.* Review of Scientific Instruments, 76, 021301-doi:10.1063/1.1854197. (2005).

Lou M., Shalev E., and Malin P.E.: *Shear-wave splitting and fracture alignments at the Northwest Geysers, California.* Geophysical Research Letters 24.15: pp 1895-1898. (1997).

Rial, J.A., Maya E., and Ming Y.: *Shear-wave splitting as a tool for the characterization of geothermal fractured reservoirs: Lessons learned.* Geothermics 34.3 : pp 365-385. (2005).

Crampin, S, and Yuan G.: *A review of techniques for measuring shear-wave splitting above small earthquakes.* Physics of the Earth and Planetary Interiors 159.1-2: pp 1-14. (2006).

Sato, M., Matsumoto, N., and Niitsuma, H.: *Evaluation of geothermal reservoir cracks by shear-wave splitting of acoustic emission.* Geothermics, 20(4), pp 197-206. (1991).